DOI: 10.1002/ejic.201000243

Synthesis, Chirality and Complexation Phenomena of Two Diastereoisomeric Dinuclear Lanthanide(III) Complexes

Benjamin S. Murray,[a] David Parker,*[a] Cidália M. G. dos Santos,[b] and Robert D. Peacock[c]

Keywords: Lanthanides / Europium / Luminescence / Chirality

Two diastereoisomeric ditopic ligands have been synthesised by linking (*SSS*)-heptadentate triamide derivative of cyclen with a central (*SS*)- or (*SR*)-1,2-diphenyl-1,2-diaminoethane derivative. Complexes of selected Ln^{III} ions (Ln = Eu, Tb, Yb) have been characterized and circularly polarised luminescence spectra of the Eu systems revealed significant differences, consistent with a change in overall complex chirality associated with the local helicity at the metal centre. Stepwise binding constants for the formation of 1:1 and 2:1 ternary adducts with (*S*)-lactate and (*S*)-*O*-phospho-tyrosine have been determined by least-squares analysis of spectral titration data, and emission and ^{1}H NMR spectroscopic data compared with the mononuclear analogue.

Introduction

Metal complexes of dinucleating ligands may afford unpredictable physical properties or chemical selectivity profiles, as a consequence of specific interactions involving each metal centre. Within the domain of lanthanide coordination complexes, examples have been reported of dinuclear complexes of Gd^{III}, assessing their utility as contrast agents in MRI.[1,2] Related work has examined the anion complexation behaviour of ditopic systems, based on two heptadentate moieties, seeking unusual binding affinities for dianions such as dicarboxylates.[3,4] Other studies have sought evidence for co-operativity in the catalysis of phosphate diester cleavage, using dinuclear complexes of Eu^{III}.[5]

Neutral heptadentate macrocyclic ligands form tripositive complexes with Ln^{III} ions in aqueous solution, and the coordination at the metal is typically made up to nine by binding to water or certain counter-anions. The affinity of such complexes for a given anion can be modulated by variation of the structure of the ligand substituent and the selection of the Ln^{III} ion. Using the chiral ligand, $\mathbf{L^1}$, for example, anion affinity profiles have been assessed in detail,[6–9] and adducts characterised by crystallography and NMR spectroscopy.[10,11] A particular aspect of this work was the chemoselectivity profile exhibited by $[Eu{\cdot}\mathbf{L^1}]^{3+}$, where a marked preference for certain phospho-anions was found,[8,9] notably with a 30:1 selectivity for *O*-phospho-tyrosine over phosphorylated serine and threonine amino acid residues.

In seeking to extend the scope of such complexes as emissive probes, ditopic systems based on $\mathbf{L^1}$ were envisaged that might allow simultaneous binding to two *O*-phospho-tyrosine sites. This could occur in a suitable peptide where the two phosphorylated residues are close in space, either by virtue of their constitution, e.g. (1,2) systems or as a result of the local helicity of the peptide chain, e.g. residues in a (1,4) or (1,5) relationship within an α-helical segment. In favourable circumstances, this might allow regioselective binding of the ditopic lanthanide complex to selected phospho-tyrosine sites. NMR Studies of the binding of $[Eu{\cdot}\mathbf{L^1}]^{3+}$ to the [5, 9, 10] triphosphorylated insulin-receptor dodecapeptide fragment revealed evidence for regioselective binding to the phosphorylated Tyr in the 9-position.[8] In related work, achiral dinuclear complexes of zinc(II) have been studied that are designed to bind simultaneously to two phospho-Tyr residues groups on proximate amino acids.[12]

Here, we report a concise synthetic approach to such systems, together with an assessment of the overall chirality of the complex and a preliminary assessment of anion affinity. The first step in this task was to prepare the ditopic ligands $\mathbf{L^{2a}}$ and $\mathbf{L^{2b}}$. In each case, the denticity of the ligand $\mathbf{L^1}$ is conserved at the macrocyclic binding site, with a common (*SSS*)-configuration at each of the stereogenic carbon centres. The linking group possess either an (*SS*)- or (*SR*)-configuration generating a pair of diastereoisomers (Figure 1). The configuration of the short, rigid linking moiety determines the preferred conformation of the derived dinuclear complexes, with the (*SS*)-linker giving rise to "con-

[a] Department of Chemistry, Durham University, South Road, Durham, DH1 3LE, UK
E-mail: david.parker@durham.ac.uk
[b] School of Chemistry, Trinity College Dublin, Dublin 2, Ireland
[c] Department of Chemistry, Glasgow University, Glasgow, G12 8QQ, UK

cave" complexes. The (*SR*)-isomer was envisaged to form an open structure, more typical of the rather flexible, achiral ditopic systems that have been explored previously.[3–5]

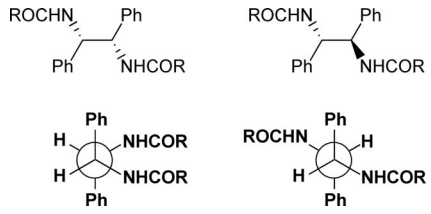

Figure 1. Newman projections of (*SS*)-$\mathbf{L^{2a}}$ (left) and (*SR*)-$\mathbf{L^{2b}}$ highlighting likely preferred conformations based on steric demand.

Ligand and Complex Synthesis and Characterization

The synthesis of each ligand was undertaken from the common intermediate, **1**, that was previously reported in studies of emissive intracellular probes.[13] Reaction of two equivalents of (*SS*)-1,2-diphenyl-1,2-diaminoethane with **1**, in the presence of EDC led to formation of **2a** in 75% yield. The same reaction with the (*SR*)-isomer did not proceed to completion and the more reactive uronium coupling agent, TBTU, was required to drive the reaction to completion and allow the desired product **2b** to be isolated (Scheme 1). Subsequent removal of the Boc protecting groups allowed $\mathbf{L^{2a}}$ and $\mathbf{L^{2b}}$ to be isolated in protonated form, as their trifluoroacetate salts. The differing stereotopism of ligand hydrogens was evident in ^{1}H NMR spectra (Figure 2). With $\mathbf{L^{2a}}$, the methine resonances of the linking moiety are homotopic, and resonate as a doublet by virtue of coupling to the vicinal amide proton. The two amide protons associated with the ring pendant arms are non-equivalent and two amide NH multiplets are observed, as each ring is rendered equivalent by the C_2-axis. With $\mathbf{L^{2b}}$, the linker methine resonances are diastereotopic and give rise to a pair of overlapping doublet of doublets. In addition, four amide NH resonances are observed for the NH protons of the ring amide substituents.

Complexation of $\mathbf{L^{2a}}$/$\mathbf{L^{2b}}$ with lanthanide(III) ions required rather forcing conditions to drive the reaction to

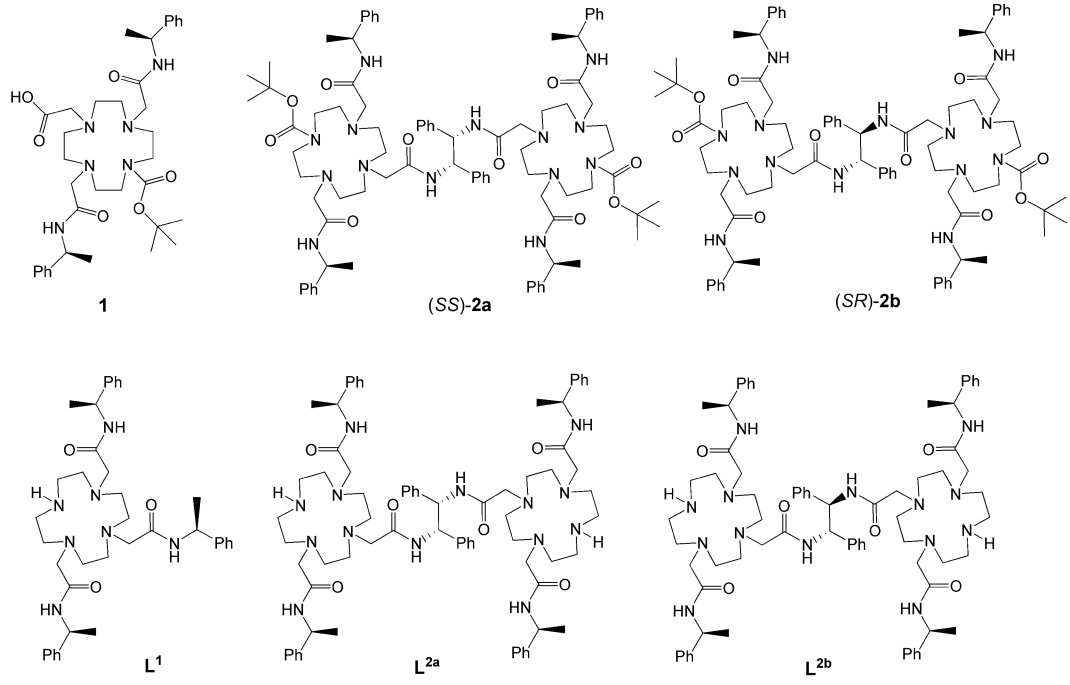

Scheme 1.

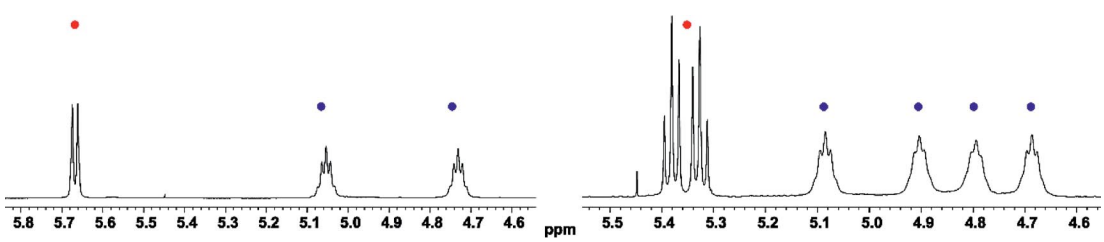

Figure 2. Partial ^{1}H NMR spectra of (*SS*)-$\mathbf{L^{2a}}$ (left) and (*SR*)-$\mathbf{L^{2b}}$ (TFA salt, 3 mM; 700 MHz, 295 K) highlighting the homotopic methine protons of the linker (δ_H = 5.67 ppm) for $\mathbf{L^{2a}}$, and the corresponding diastereotopic methine protons about 5.35 ppm for $\mathbf{L^{2b}}$. For $\mathbf{L^{2a}}$, two C*H*Me multiplets are observed, whereas for $\mathbf{L^{2b}}$ each C*H*Me proton is non-equivalent.

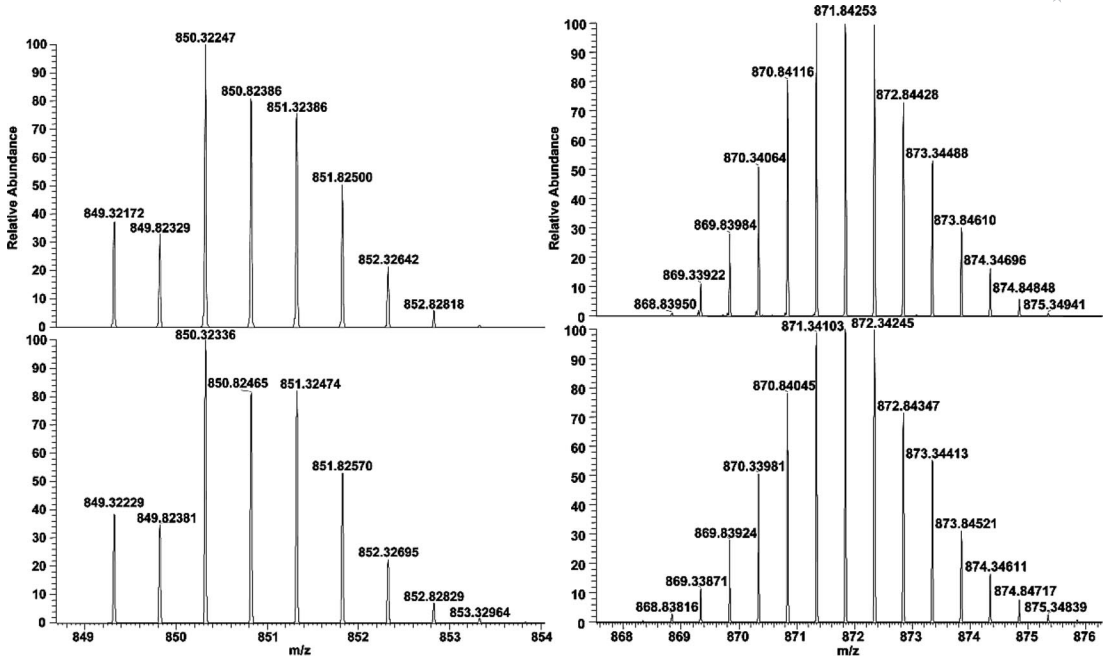

Figure 3. Observed (*top*) and experimental (*bottom*) mass spectral isotope patterns for diacetate adducts of $[Eu_2{\cdot}\mathbf{L^{2a}}]^{6+}$ (*left*; $[M + 2OAc - 2H]^{2+}$) and $[Yb_2{\cdot}\mathbf{L^{2b}}]^{6+}$ (*right*, $[M + 2OAc - 2H]^{2+}$).

completion. Typically, six equivalents of $Eu(CF_3SO_3)_3$, $TbCl_3$ or $Yb(OAc)_3$ was used. Excess salt was removed by dialysis, using benzoylated dialysis tubing with a 2000 MW cut-off. Where appropriate, ion exchange chromatography, led to isolation of the water-soluble chloride salt. Analysis of the product by HPLC and electrospray mass spectrometry confirmed that complexation had proceeded to completion. Mass spectral analyses were carried out in the presence of the weak acid ammonium acetate, and gave rise to characteristic isotope patterns for the di-acetate salts of the given complex (Figure 3). Adducts were detected as either triply or doubly charged species, formed through the loss of either one or two protons.[14] In every case, two acetate anions were associated with the complex, suggesting that in the observed species, each metal centre is bound to one acetate anion. Previously, the crystal structure of $[Yb{\cdot}\mathbf{L^1}(OAc)]^{2+}$ has been reported, revealing acetate chelation at the Yb centre.[10]

Proton NMR spectra of the Yb and Eu^{III} complexes of $\mathbf{L^{2a}}$ and $\mathbf{L^{2b}}$ were examined as their chloride salts (500 MHz, 295K D_2O 2 mM complex) and revealed significant differences between the isomers. Spectra of $[Eu_2{\cdot}\mathbf{L^{2b}}]^{6+}$ and $[Yb_2{\cdot}\mathbf{L^{2b}}]^{6+}$ were found to be the simplest, with one major species evident in which the paramagnetically shifted protons of the two macrocycles were non-equivalent. With $[Eu_2{\cdot}\mathbf{L^{2a}}]^{6+}$ and $[Yb_2{\cdot}\mathbf{L^{2a}}]^{6+}$, two species were observed (ratio 3:1) for each of which a similar number of paramagnetically shifted resonances was observed. No particular spectral simplification was observed at 278 K, and at 323 K significant line-broadening was evident.

Total emission and circularly polarised luminescence (CPL) spectra were recorded for $[Eu_2{\cdot}\mathbf{L^{2a}}]^{6+}$ and $[Eu_2{\cdot}\mathbf{L^{2b}}]^{6+}$. The form of the metal-based total emission spectrum was virtually identical, consistent with the presence of a common coordination environment around each Eu^{III} centre.[6,15] Circularly polarised emission spectroscopy is used to probe the chirality of the metal excited state, offering advantages of sensitivity over ground state CD studies.[15] The CPL spectra of $[Eu{\cdot}\mathbf{L^1}]^{3+}$ and (*SR*)-$[Eu_2{\cdot}\mathbf{L^{2b}}]^{6+}$ were very similar (Figure 4) but that of (*SS*)-$[Eu_2{\cdot}\mathbf{L^{2a}}]^{6+}$ was significantly different and much weaker in intensity, especially in the electric-dipole allowed $\Delta J = 2$ transitions around 612 nm. Various emission dissymmetry factors (g_{em}) were recorded (Table 1). For certain transitions, the sign of the observed CPL was opposite for $[Eu_2{\cdot}\mathbf{L^{2a}}]^{6+}$ compared to $[Eu_2{\cdot}\mathbf{L^{2b}}]^{6+}$ and $[Eu{\cdot}\mathbf{L^1}]^{3+}$. The differences strongly suggest that opposite local helicities exist at the two Eu centres in $[Eu_2{\cdot}\mathbf{L^{2a}}]^{6+}$. This leads to a reduced overall CPL. In contrast, the CPL spectrum for $[Eu_2{\cdot}\mathbf{L^{2b}}]^{6+}$ is consistent with each Eu centre behaving independently and identically to the mononuclear complex, $[Eu{\cdot}\mathbf{L^1}]^{3+}$. Given that the X-ray structure of the diaqua complex (*SSS*)-$[Eu{\cdot}\mathbf{L^1}(OH_2)_2]^{3+}$-$(CF_3SO_3)_3$ has been determined, confirming the presence of a nine-coordinate complex with a Δ configuration, and that the CPL analysis in solution has been shown to be consistent with this assignment,[7,15] such behaviour accords with the hypothetical conformational analysis presented above (Figure 1).

The excited state radiative lifetimes of the Eu and Tb^{III} complexes were measured in H_2O and D_2O, and in the presence of selected anions (Table 2) in order to deduce apparent hydration states, q.[16] The chloride salts of Eu/Tb gave q values in the range 1.3 to 1.4, notably lower than the values of 2.1 observed with $[Ln{\cdot}\mathbf{L^1}]^{3+}$.[6] Such behaviour could indicate the presence of two isomeric complexes of differing hydration number, associated with the increased

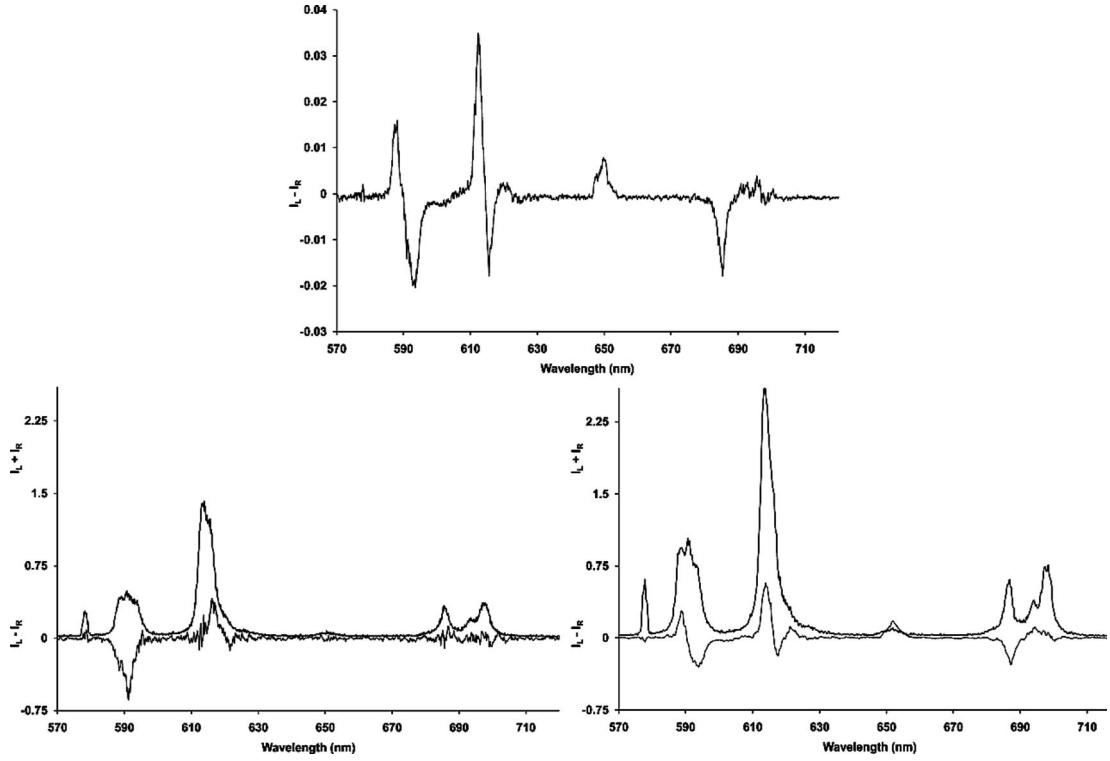

Figure 4. Circularly polarised luminescence (CPL) spectra for $[Eu{\cdot}\mathbf{L^1}]^{3+}$ (*top*) compared to $[Eu_2{\cdot}\mathbf{L^{2a}}]^{6+}$ (*left*) and $[Eu_2{\cdot}\mathbf{L^{2b}}]^{6+}$ (*right*) (295 K, D_2O, 1 mM, λ_{ex} = 255 nm). The CPL spectra are scaled by a factor of 18 compared to the total emission spectra.

Table 1. Emission disymmetry values g_{em} from CPL spectra (D_2O, 295 K, λ_{exc} = 397 or 255 nm).

Complex	Observed transition		
	ΔJ = 1 (588 nm)	ΔJ = 1 (592 nm)	ΔJ = 2 (613 nm)
$[Eu{\cdot}\mathbf{L^1}]^{3+}$	+0.04	–0.05	+0.03
$[Eu_2{\cdot}\mathbf{L^{2a}}]^{6+}$	–0.03	–0.03	+0.003
$[Eu_2{\cdot}\mathbf{L^{2b}}]^{6+}$	+0.03	–0.05	+0.025

hydrophobicity of the ditopic ligands, $\mathbf{L^{2a}}$ and $\mathbf{L^{2b}}$ compared to $\mathbf{L^1}$. Addition of a ten-fold excess of (*S*)-lactate and (*S*)-*O*-phospho-tyrosine to the terbium complexes of $\mathbf{L^{2a}}$/$\mathbf{L^{2b}}$ gave rise to complete and partial water displacement respectively, with apparent hydration numbers of a similar magnitude to those measured for $[Tb{\cdot}\mathbf{L^1}]^{3+}$.[6] In the latter case, it has been unequivocally demonstrated that the lactate anion chelates to the lanthanide centre, displacing water and that phospho-anions, such as *O*-phospho-Tyr, form a ternary adduct where one water molecule remains weakly bound.[5,6,17]

Table 2. Rate constants *k* for the decay of the excited states of europium(III) and terbium(III) complexes and derived apparent hydration states *q* in the presence of the stated anion [295 K, 50 μM complex, 500 μM anion (Na^+ or K^+ salt), λ_{exc} = 397 or 255 nm].

Complex/anion	k_{H2O}/ms^{-1}	k_{D2O} /ms^{-1}	q (± 20%)
$[Eu_2{\cdot}\mathbf{L^{2a}}]^{6+}/Cl^-$	2.78	1.22	1.3
$[Eu_2{\cdot}\mathbf{L^{2b}}]^{6+}/Cl^-$	2.86	1.22	1.4
$[Tb_2{\cdot}\mathbf{L^{2a}}]^{6+}/Cl^-$	0.72	0.47	0.9
$[Tb_2{\cdot}\mathbf{L^{2b}}]^{6+}/Cl^-$	0.79	0.48	1.2
$[Tb_2{\cdot}\mathbf{L^{2a}}]^{6+}$/lactate	0.58	0.49	0.1
$[Tb_2{\cdot}\mathbf{L^{2b}}]^{6+}$/lactate	0.59	0.47	0.3
$[Tb_2{\cdot}\mathbf{L^{2a}}]^{6+}$/OPTyr	0.77	0.65	0.3
$[Tb_2{\cdot}\mathbf{L^{2b}}]^{6+}$/OPTyr	0.68	0.49	0.6

Anion Binding Revealed by NMR and CPL Emission Studies

Incremental addition of various anions to $[Yb_2{\cdot}\mathbf{L^{2a}}]^{6+}$ was monitored by ^1H NMR spectroscopy. Analysis of the data was hampered by considerable line broadening (500 MHz, 295 K) and by the tendency of certain anions to induce precipitation. Such behaviour had not been evident with the mononuclear system $[Yb{\cdot}\mathbf{L^1}]^{3+}$.[8,9] Accordingly, only a restricted set of anions could be studied. ^1H NMR spectra for the dinuclear Yb complexes of $\mathbf{L^{2a}}$/$\mathbf{L^{2b}}$ were recorded in the presence of ten equivalents of tyrosine, *O*-phospho-tyrosine and hydrogen carbonate (Figure 5). This allowed a comparison with the spectrum of the aqua complex, obtained with a chloride counterion that does not coordinate to the metal ion. Spectral analysis focused on the behaviour of the most paramagnetically shifted "axial" ring proton, H_{ax}, resonating to higher frequency of all other resonances. The mean chemical shift of this resonance is a sensitive reporter of the lanthanide(III) coordination environment, particularly the nature and polarisability of the "capping" axial donor substituent, in the mono-capped square antiprismatic coordination environment.[18,19] Mean chemical shift values obtained, for H_{ax} (Table 3) highlight the dif-

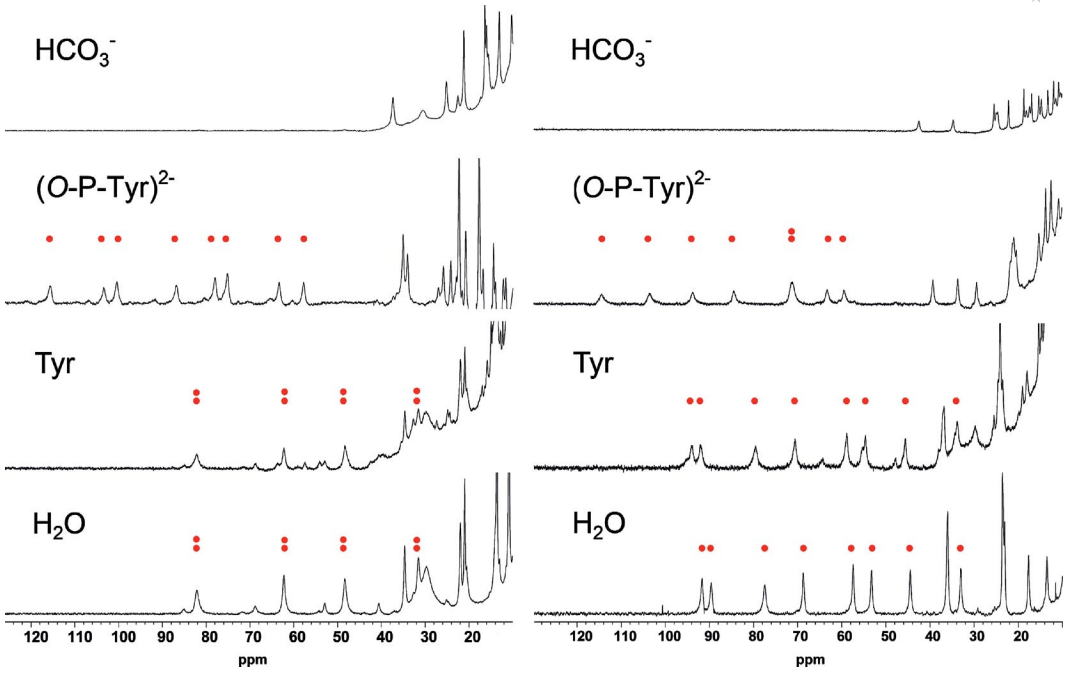

Figure 5. Partial ^{1}H NMR spectra (500 MHz, D_2O, 295 K, pD 7.8, 2 mM complex) of chloride salts of $[Yb_2{\cdot}\mathbf{L^{2a}}]^{6+}$ (*left*) and $[Yb_2{\cdot}\mathbf{L^{2b}}]^{6+}$ (*right*) in the presence of the indicated anions (10 mM) highlighting the formation of ternary adducts with HCO_3^- and *O*-phospho-Tyr only.

ferences between $[Yb{\cdot}\mathbf{L^1}]^{3+}$ and the dinuclear complexes. For example, addition of tyrosine does not significantly perturb the NMR spectrum of the dinuclear Yb, aqua species, whereas with $[Yb{\cdot}\mathbf{L^1}]^{3+}$ an "N–O" chelate was formed under these conditions, with displacement of bound water; the mean chemical shift value for H_{ax} was 36 ppm.[8,9,11] Such a chelated species, with an "axial" coordinated amino group (evident in related X-ray analyses[11]) was also a competitive binding mode in complexation of $[Yb{\cdot}\mathbf{L^1}]^{3+}$ with *O*-phospho-Tyr. This behaviour was not evident for each dimeric complex (Figure 5) and the value of δ_{ax}^{mean} was consistent with selective monodentate phosphate ligation. A further feature was evident in the behaviour of $[Yb_2{\cdot}\mathbf{L^{2a}}]^{6+}$. In the aqua complex, one major species was observed, in which the H_{ax} resonances for each ring appeared to be chemical shift equivalent (Figure 5). In the *O*-phospho-Tyr adduct this shift-equivalence was removed, and four resonances for the H_{ax} protons in each 12-N-4 ring were clearly discerned.

Table 3. Selected ^{1}H NMR chemical shift data for ternary anion adducts (295 K, pD = 7.8, 500 MHz; 2 mM complex, 10 mM stated anion) examining the mean value for the most shifted ring proton.[a]

Complex	Anion/mean δ_H (ppm) for H_{ax}		
	Cl^- or $CF_3SO_3^-$	*O*-phospho-Tyr	Tyr
$[Yb{\cdot}\mathbf{L^1}]^{3+}$	75	95(40)	39
(*SS*)-$[Yb_2{\cdot}\mathbf{L^{2a}}]^{6+}$	56	85	55[b]
(*SR*)-$[Yb_2{\cdot}\mathbf{L^{2b}}]^{6+}$	65	80	64[b]

[a] Values for minor species are given in parenthesis. [b] Data suggest that the aqua species remains present, with little or no evidence for coordination of the tyrosine carboxylate or primary amine group.

Addition of hydrogen carbonate caused significant contraction of the ^{1}H NMR spectral width for each Yb complex, consistent with a reduction in the second order crystal field coefficient that determines the size of the paramagnetic dipolar shift. Chelation of carbonate at each metal centre replaces the "hard" water molecule with a more polarisable charged oxygen donor in the "axial" capping site.[14,18] Binding of inorganic phosphate to the Eu and Yb complexes of $\mathbf{L^{2a}}$/$\mathbf{L^{2b}}$ led to precipitation, inhibiting spectral studies. However, the addition of glucose-6-phosphate and glucose-1,6-diphosphate did not cause any solid to form, permitting ^{1}H NMR and CPL spectral studies. ^{1}H NMR spectra of $[Eu_2{\cdot}\mathbf{L^{2b}}]^{6+}$ recorded in the presence of these anions were sharp and resembled those obtained under the same conditions with $[Eu{\cdot}\mathbf{L^1}]^{3+}$; the number of resonances observed was consistent with formation of a dinuclear *O*-phospho-bound ternary adduct, in which each metal centre is non-equivalent. With $[Eu_2{\cdot}\mathbf{L^{2a}}]^{6+}$, the addition of glucose-1,6-diphosphate gave rise to a spectrum with broad resonances, possibly due to the formation of 1:1 and 2:1 adducts in intermediate exchange on the NMR timescale. CPL spectra of the dinuclear europium aqua complexes, in the absence and presence of the phosphorylated glucose species, were also obtained (Figure 6). Spectra for $[Eu_2{\cdot}\mathbf{L^{2b}}]^{6+}$ resembled those obtained with $[Eu{\cdot}\mathbf{L^1}]^{3+}$,[9a] consistent with a common Δ-configuration at both Eu centres in each species. In contrast, CPL spectra for $[Eu_2{\cdot}\mathbf{L^{2a}}]^{6+}$ (Figure 6, upper part) were very weak and differed in sign for the $\Delta J = 1$, magnetic-dipole allowed transitions observed. Such behaviour suggests that the local helicities at the two Eu centres in $[Eu_2{\cdot}\mathbf{L^{2b}}]^{6+}$ are of opposite

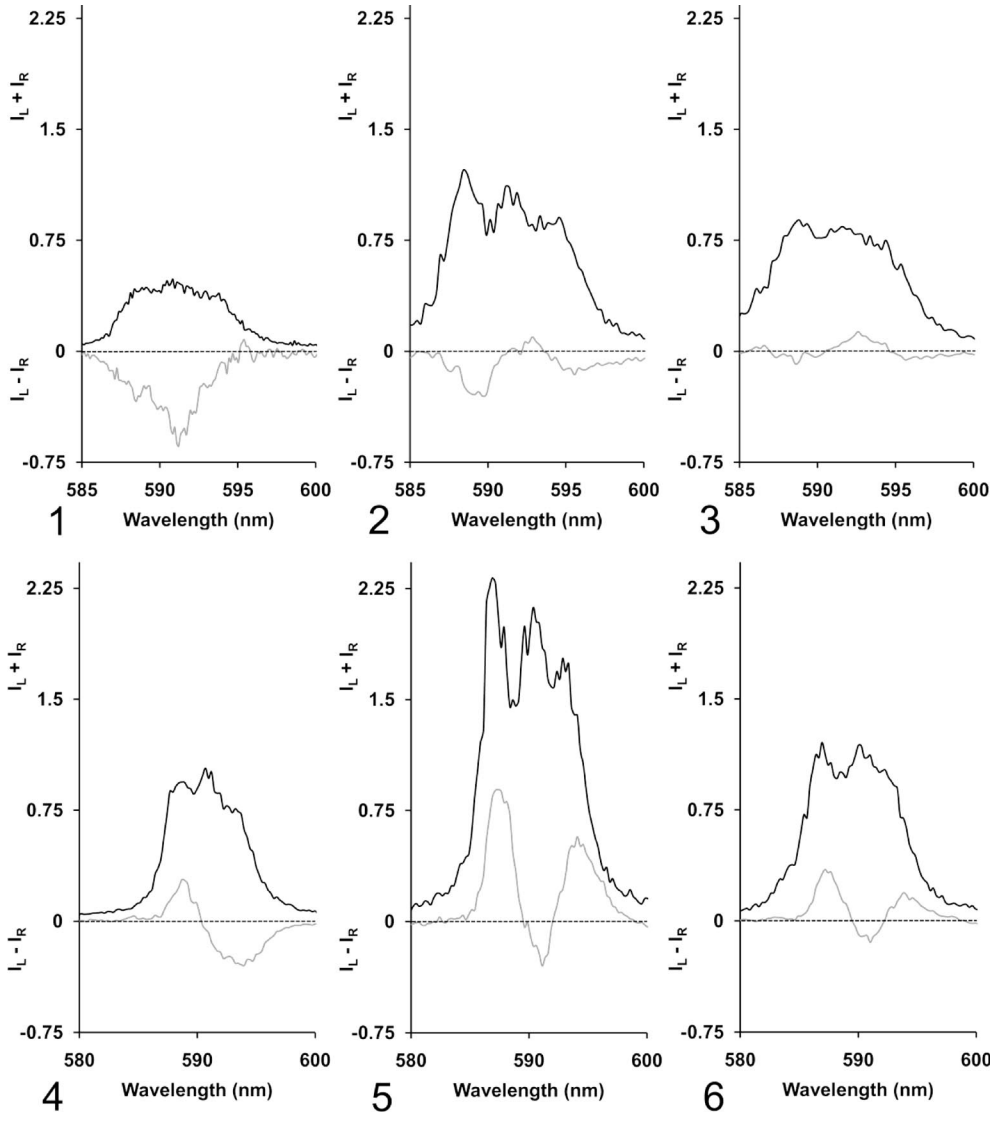

Figure 6. CPL spectra (1 mM complex, D_2O, 295 K, λ_{exc} 255 nm) highlighting the magnetic-dipole-allowed $\Delta J = 1$ transitions for: 1) $[Eu_2{\cdot}\mathbf{L^{2a}}]^{6+}$; 2) $[Eu_2{\cdot}\mathbf{L^{2a}}]^{6+}$/10 eqs glucose-6-phosphate; 3) $[Eu_2{\cdot}\mathbf{L^{2a}}]^{6+}$/10 eqs glucose-1,6-diphosphate; 4) $[Eu_2{\cdot}\mathbf{L^{2b}}]^{6+}$; 5) $[Eu_2{\cdot}\mathbf{L^{2b}}]^{6+}$/10 eqs glucose-6-phosphate; 6) $[Eu_2{\cdot}\mathbf{L^{2b}}]^{6+}$/10 eqs glucose-1,6-diphosphate. For 1) to 3) CPL spectra are $\times 60$ with respect to the shown total emission spectra; = for 4) to 6) this factor is $\times 18$.

sense, consistent with the presence of $\Delta(\lambda\lambda\lambda\lambda)$ and $\Lambda(\delta\delta\delta\delta)$ stereoisomeric species, specifying the elements of chirality associated with the ligand NCCO and NCCN torsion angles, respectively.[14,18]

Analysis of Luminescence Spectral Titrations

The tyrosine chromophore is well known to sensitise the terbium emission efficiently.[20] Accordingly, binding of *O*-phospho-Tyr to the Tb complexes of $\mathbf{L^1}$, $\mathbf{L^{2a}}$ and $\mathbf{L^{2b}}$ was monitored following excitation at 275 nm, observing modulation of terbium emission intensity at 545 nm. Job plots were used to establish the 1:1 stoichiometry of association of *O*-phospho-Tyr with $[Tb{\cdot}\mathbf{L^1}]^{3+}$, and the 2:1 stoichiometry for the dinuclear systems (Figure 7). Spectral titrimetric data were analysed using least-squares fitting methods, associated with SPECFIT,[21,22] based on successive 1:1 and 2:1 binding models (Table 4). The binding curve for association of *O*-phospho-Tyr with $[Tb_2{\cdot}\mathbf{L^{2a}}]^{6+}$ and $[Tb_2{\cdot}\mathbf{L^{2b}}]^{6+}$ (Figure 7, centre/upper, left) reached a maximum after addition of two equivalents of the phospho-anion, consistent with the Job plot data (not shown). Lower values for the stability of the 1:1 and 2:1 adducts were found for $[Tb_2{\cdot}\mathbf{L^{2a}}]^{6+}$ compared to $[Tb_2{\cdot}\mathbf{L^{2b}}]^{6+}$, consistent with the more open structure in the latter case, in which the metal centres behave independently. With $[Tb_2{\cdot}\mathbf{L^{2a}}]^{6+}$, the more concave structure may lead to some degree of steric inhibition of anion binding.

A similar series of titrations was undertaken with the (*S*)-lactate anion (Table 4). Estimated affinity constants were lower than for *O*-phospho-Tyr, consistent with the less favourable electrostatic contribution to the free energy of

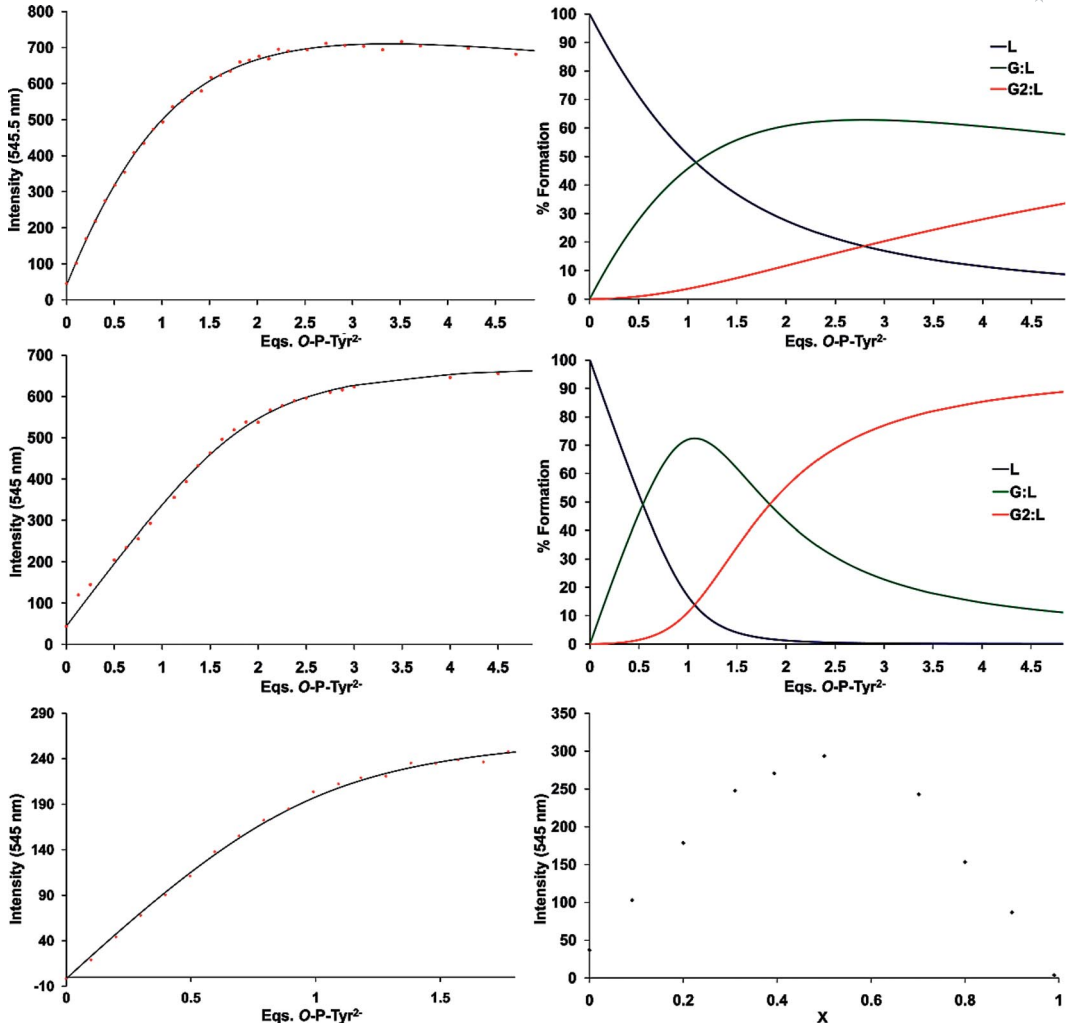

Figure 7. Binding curves (*left*) and equilibrium species distribution diagrams (*right*) characterising complexation of terbium complexes with *O*-phospho-tyrosine (295 K, pH 7.4, λ_{exc} 275 nm). *Top*: $[Tb_2{\cdot}\mathbf{L^{2a}}]^{6+}$ (50 μM); *centre*: $[Tb{\cdot}\mathbf{L^{2b}}]^{6+}$ (50 μM); *bottom*: $[Tb{\cdot}\mathbf{L^{1}}]^{3+}$ (110 μM). The Job plot, is consistent with 1:1 stoichiometry of complexation for $[Tb{\cdot}\mathbf{L^{1}}]^{3+}$/*O*-phospho-Tyr.

Table 4. Formation constants for association of Tb^{III} complexes with (*S*)-lactate and *O*-phospho-(*S*)Tyr (295 K, pH 7.4).[a]

Complex	[lactate]$^-$		[*O*-phospho-Tyr]$^{2-}$	
	$\log\beta_{ML}$	$\log\beta_{ML2}$	$\log\beta_{ML}$	$\log\beta_{ML2}$
$[Tb{\cdot}\mathbf{L^{1}}]^{3+}$	3.80(0.01)	–	4.88(0.10)	–
$[Tb_2{\cdot}\mathbf{L^{2a}}]^{6+}$	4.50(0.10)	7.70(0.27)	4.60(0.03)	8.14(0.10)
$[Tb_2{\cdot}\mathbf{L^{2b}}]^{6+}$	4.58(0.13)	7.60(0.19)	5.67(0.30)	10.45(0.29)

[a] Defining "M" as the Tb complex, and "L" as the anion, with standard deviations in parenthesis.

binding for the mono-anion lactate, offset somewhat by the more favourable energy term associated with lactate chelation and displacement of bound water.[10] The $\log\beta$ values for each stereoisomeric terbium complex were similar in magnitude, suggesting a lesser role for any steric effect. The 1:1 formation constant for $[Tb{\cdot}\mathbf{L^{1}}]^{3+}$ was lower than for the dinuclear systems, consistent with a bigger electrostatic binding energy term, as a result of the greater positive charge of the latter systems.

Summary and Conclusions

The dinuclear lanthanide(III) complexes of the stereoisomeric ligands $\mathbf{L^{2a}}$ and $\mathbf{L^{2b}}$ possess different local helicities at the metal centre as revealed by the CPL studies. This can be attributed to their differing solution conformations, dictated by the configuration of the linking moiety. The structure of the dinuclear complexes of (*SS*)-$\mathbf{L^{2a}}$ must be concave, leading to the creation of local metal helicities of opposite sign. With the complexes of (*SR*)-$\mathbf{L^{2b}}$, the CPL and solution complexation behaviour echo the behaviour of the mononuclear complex of $\mathbf{L^{1}}$; thus, the two metal centres in $[Ln_2{\cdot}\mathbf{L^{2b}}]$ behave independently.

The high positive charge of these dinuclear complexes leads to the formation of rather insoluble complexes with several anions (e.g., HPO_4^{2-}, ATP^{4-}) curtailing more detailed analyses. Future work on such systems will embrace more hydrophilic derivatives, obtained by introducing sulfonate or carboxylate groups into either the two central or the four peripheral aryl rings. It is more likely that the concave

systems based on the (*SSS*)-mononuclear complex linked by an (*SS*)-diamide sub-unit, i.e., $\mathbf{L^{2a}}$ will give rise to the desired chemoselectivity for (1,4)- or (1,5)-di-phosphorylated species. The diastereoisomeric complexes of $\mathbf{L^{2b}}$ may serve simply as a cross-linking agent between two anion binding sites.

Experimental Section

Determination of Binding Constants: To examine the influence of some biologically common anions on complexes, titrations were carried out examining separate solutions containing either *O*-phospho-(*S*)-tyrosine or sodium (*S*)-lactate. Each measurement was carried out by adding the anion as a concentrated stock solution such that the incremental volume change was 0.1–0.5% of the original solution volume, thereby avoiding any significant increase in sample volume. At each stage the pH was corrected to 7.40 (±0.04) by using either concd. aqueous HCl or sodium hydroxide solution. Each emission spectrum was corrected for dilution.

Every binding constant was calculated using the non-linear least-squares programme SPECFIT/32™.[21] The fitting methodology, which relies on the use of various mathematical parameters, uses the Levenberg–Marquardt procedure to minimise the least-squares residuals between the data set and the model system.[22]

Reverse-Phase HPLC and Dialysis: Reverse phase HPLC analyses were performed at 298 K using a Perkin–Elmer Series 200 set up, with a diode array and fluorescence detector. A Phenomenex Synergi Fusion RP 80 Å analytical column (4.6 mm × 150 mm; 4 μm) was used with a flow rate of 1 mL min^{-1}. The solvent system used had the following time profile, with linear solvent gradient for the period 5 to 25 min: 0–5 min: 100% 0.1% TFA in water; 5 to 20 min: 100% of 0.1% TFA/water declining to 0% with 0.1% TFA/MeCN rising over the same time interval; 20.1 to 2 5 min: return to start with 100% water/0.1% TFA.

Excess $LnCl_3$ or $Ln(OAc)_3$ salts were removed from the dinuclear complexes of $\mathbf{L^{2a}}$ and $\mathbf{L^{2b}}$ using benzoylated dialysis tubing (9 mm flat width, MWCO 2000) (Sigma–Aldrich). Typically the dialysis tubing was washed with H_2O, the solid complex was dissolved in H_2O (1 mL) and the solution was transferred to the tubing that was sealed by clamping at both ends. The tubing was submerged in stirring H_2O (500 mL) and the H_2O was exchanged four times over 72 h followed by the removal and filtering of the tubing contents. The aqueous solution was then frozen and lyophilized to yield the desired complex.

Emission and CPL Spectroscopy: Emission spectra were recorded with a Fluorolog-3 spectrofluorimeter; CPL spectra were recorded with a custom-modified Spex Fluoromax-2 spectrometer at the University of Glasgow.

Synthetic Procedures

[7-(*tert*-Butoxycarbonyl)-4,10-bis(2-oxo-2-{[(1*S*)-1-phenylethyl]-amino}ethyl)-1,4,7,10-tetraazacyclododecan-1-yl]acetic Acid (1): This intermediate was synthesised as described in the literature.[13]

Di-*tert*-butyl 7,7′-{[(1*S*,2*S*)-1,2-Diphenylethane-1,2-diyl]bis[imino(2-oxoethane-2,1-diyl)]}bis[4,10-bis(2-oxo-2-{[(1*S*)-1-phenylethyl]-amino}ethyl)-1,4,7,10-tetraazacyclododecane-1-carboxylate] (2a): Compound **1** (0.166 g, 0.254 mmol), EDC·HCl (0.054 g, 0.282 mmol), HOBt (10 mg) and NEt_3 (0.1 mL, 0.717 mmol) in $CHCl_3$ (5 mL) were stirred at room temperature. After 25 min (1*S*,2*S*)-(–)-1,2-diphenylethylenediamine (0.024 g, 0.113 mmol) was added to the solution which was stirred for a further 10 h then washed with satd. $NaHCO_{3\ (aq)}$ (10 mL) followed by H_2O (10 mL). The clear organic solution was dried, solvent removed under reduced pressure and the residue purified by column chromatography (alumina using a DCM/MeOH solvent system starting from 100% DCM then increasing the volume of MeOH by 0.5% every 50 mL thereafter) to yield the desired product as a clear glassy solid (0.126 g, 0.085 mmol, 75%); R_F (Alumina, DCM/MeOH, 99:1): 0.80; m.p. 89–91 °C. ^{1}H NMR ($CDCl_3$, 400 MHz): δ = 9.82 (br. s, 1 H, NH), 9.08 (br. s, 1 H, NH), 7.88 (br. s, 4 H, arm NH), 7.18–7.28 (br. m, 30 H, arm and linker Ar protons), 5.39 and 5.53 (br. s, 2 H, linker CH), 5.01 (br. s, 4 H, arm CH), 2.03–3.30 (br. m, 44 H, cyclen CH_2, amide arm CH_2CO and linker CH_2CO), 1.39 (br. m, 30 H, amide arm CH_3 and *t*Bu CH_3) ppm. ^{13}C NMR ($CDCl_3$, 100 MHz): δ = 170.8 (br. m, 6 C, amide arms C=O and linker C=O), 156.1 (2 C, Boc C=O), 143.6 (6 C, amide arms and linker $Ph_{(q)}$), 128.9, 127.6, 126.6 (br., 30 C, amide arm and linker Ph), 80.0 (2 C, $Boc_{(q)}$), 46.9–62.6 (br., 24 C, cyclen CH_2, amide arm CH_2, linker CH_2 and linker stereocentre C), 28.7 (6 C, Boc CH_3), 22.3 (4 C, amide arm CH_3) ppm. MS (ES$^-$) *m*/*z* 1480.4 [M – H]$^-$ 35%, 1517.5 [M + Cl]$^-$ 50%. HRMS (ES$^+$) *m*/*z* found 1481.910 [M + H]$^+$ $C_{84}H_{117}O_{10}N_{14}$ requires 1481.907.

Ligand $\mathbf{L^{2a}}$: A colourless solution of **2a** (0.093 g, 0.063 mmol) in DCM/TFA (50:50, 5 mL) was stirred for 12 h in a sealed flask. The resultant yellow-tinged solution was dried under reduced pressure to yield the TFA salt of the desired product, as a glassy yellow solid, in quantitative yield. ^{1}H NMR (CD_3CN, 500 MHz): δ = 9.77 (d, *J* = 9.5 Hz, 2 H, cyclen NH), 7.77 (br. s, 4 H, arm NH), 7.04–7.48 (m, 30 H, arm and linker Ar), 5.67 (d, *J* = 9.0 Hz, 2 H, linker CH), 5.05 (m, 2 H, arm CH), 4.69 (m, 2 H, arm CH), 3.92 (d, *J* = 15.5 Hz, 2 H, linker CH_2), 3.71 (d, *J* = 15.5 Hz, 2 H, linker CH_2), 2.62–3.29 (m, 40 H. cyclen CH_2 and arm CH_2), 1.46 (d, *J* = 7.0 Hz, 6 H, arm CH_3), 1.24 (d, *J* = 7.0 Hz, 6 H, arm CH_3) ppm. ^{13}C NMR (CD_3CN, 125 MHz): δ = 170.7 (4 C, arm C=O), 164.4 (2 C, linker C=O), 160.4 (q, 2 C, TFA C=O), 144.7, 144.4 (4 C, arm $Ar_{(q)}$), 139.8 (2 C, linker $Ar_{(q)}$), 129.7, 129.5, 129.3, 128.8, 2 × 128.0, 127.1, 127.0 (30 C, arm and linker Ar), 115.7 (q, 2 C, TFA CF_3), 58.7 (2 C, linker CH), 56.7, 55.9, 53.0, 52.3, 51.8, 50.8, 49.1, 48.4 (16 C, cyclen CH_2), 55.4 (2 C, linker CH_2), 49.8, 49.7 (4 C, arm CH), 43.8, 43.7 (4 C, arm CH_2), 22.6, 22.1 (4 C, arm CH_3) ppm. MS (ES$^+$) *m*/*z* 641.4 [M + 2H]$^{2+}$ 100%. HRMS (ES$^+$) *m*/*z* found 641.4055 [M + 2H]$^{2+}$ $C_{74}H_{102}O_6N_{14}$ requires 641.4048.

$[Eu_2{\cdot}\mathbf{L^{2a}}(H_2O)_4]Cl_6{\cdot}xH_2O$: Compound $\mathbf{L^{2a}}$ as its TFA salt (0.082 g, 0.064 mmol, molar mass of ligand as its free base used) and $Eu(OTf)_3$ (0.230 g, 0.384 mmol) in dry MeCN (1.75 mL) were heated at reflux for 36 h under an atmosphere of argon. The solution was then cooled to room temperature followed by removal of the solvent under reduced pressure. The solid was sonicated in DCM (2 × 5 mL) followed by collection of the solid by centrifugation, decanting the DCM phase; the solid was dried under reduced pressure. The grey solid left was sonicated in water (5 mL), the water was decanted followed by the drying of the remaining solid under reduced pressure. The solid was made water soluble by the exchange of the triflate anions for chloride anions using ion exchange resin (0.2 g of DOWEX 1 × 8 200–400 mesh Cl). The crude complex was isolated from excess $EuCl_3$ using benzoylated dialysis tubing, to yield the desired product as a white powder (0.089 g, 0.047 mmol, 74%). MS (ES$^+$, excess ammonium acetate) *m*/*z* 567.1 [M + 2CH_3CO_2 – H]$^{3+}$ 95%, 850.2 [M + 2CH_3CO_2 – 2H]$^{2+}$ 100%. HRMS (ES$^+$) *m*/*z* found 849.3217 [M + 2CH_3CO_2 – 2H]$^{2+}$ $C_{78}H_{104}O_{10}N_{14}{}^{151}Eu_2$ requires 849.3223; HPLC: t_R = 8.5 min.

$[Tb_2{\cdot}L^{2a}(H_2O)_4]Cl_6{\cdot}xH_2O$: Compound L^{2a} as its TFA salt (0.017 g, 0.013 mmol, molar mass of ligand as its free base used) and $TbCl_3{\cdot}6H_2O$ (0.031 g, 0.083 mmol) in dry MeOH (1.5 mL) were heated at reflux for 36 h under argon. The solution was then cooled to room temperature followed by removal of the solvent under reduced pressure. The solid was sonicated in DCM (2 × 5 mL), the solid collected by centrifugation and the solid was dried under reduced pressure. The residual grey solid was sonicated in water (5 mL), the water decanted and the remaining solid dried under reduced pressure. The complex was isolated from excess $TbCl_3$ using benzoylated dialysis tubing (9 mm flat width) to yield the desired product as a white powder (0.020 g, 0.010 mmol, 80%). MS (ES+ with ammonium acetate) *m*/*z* 571.7 $[M + 2CH_3CO_2 – H]^{3+}$ 90%, 857.2 $[M + 2CH_3CO_2\text{-}2H]^{2+}$ 100%. HRMS (ES^+) *m*/*z* found 857.3270 $[M + 2CH_3CO_2 – 2H]^{2+}$ $C_{78}H_{104}O_{10}N_{14}{}^{159}Tb_2$ requires 857.3278; HPLC: t_R = 8.7 min.

$[Yb_2{\cdot}L^{2a}(OAc)_2]OAc_4{\cdot}xH_2O$: Compound L^{2a} as its TFA salt (0.044 g, 0.034 mmol, molar mass of ligand as free base used) and $Yb(OAc)_3{\cdot}4H_2O$ (0.086 g, 0.20 mmol) in $MeOH/H_2O$ (2 mL, 50:50) were heated at reflux for 48 h under argon. The solution was cooled to room temperature and solvent removed under reduced pressure. The complex was isolated from excess $Yb(OAc)_3$ using benzoylated dialysis tubing to yield the desired product as a white solid (0.055 g, 0.028 mmol, 82%); m.p. 191–192 °C (dec.). MS (ES^+, excess ammonium acetate) *m*/*z* 581.6 $[M + 2CH_3CO_2 – H]^{3+}$ 100%, 872.2 $[M + 2CH_3CO_2 – 2H]^{2+}$ 5%. HRMS (ES^+) *m*/*z* found 869.3400 $[M + 2CH_3CO_2 – 2H]^{2+}$ $C_{78}H_{104}O_{10}N_{14}Yb_2$ requires 869.3391; HPLC: t_R = 8.4 min.

Ligand 2b: Compound **1** (0.070 g, 0.107 mmol), TBTU (0.034 g, 0.106 mmol), $HOBt{\cdot}xH_2O$ (0.014 g, 0.104 mmol) and NEt_3 (0.03 mL, 0.215 mmol) in MeCN (1.5 mL) were stirred, under argon, at room temperature for 15 min followed by the addition of *meso*-1,2-diphenylethylenediamine (0.011 g, 0.052 mmol). The pale yellow solution was stirred at room temperature for 24 h followed by removal of solvent under reduced pressure. The remaining yellow residue was taken up in DCM (10 mL) to give a solution that was washed with $HCl_{(aq)}$ (0.1 M, 20 mL), satd. $NaHCO_3$ (10 mL) then H_2O (10 mL). The organic solution was concentrated to a volume of 1 mL under reduced pressure then dripped into cold diethyl ether (15 mL). The pale yellow precipitate was collected by centrifugation and dried under reduced pressure to yield a cream coloured powder (0.042 g, 0.028 mmol, 54%); m.p. 92–94 °C. ^1H NMR ($CDCl_3$, 500 MHz): δ = 7.73 (br. s, 1 H, amide NH), 7.14–7.29 (br. m, 35 H, arm and linker Ar protons and amide NH), 5.40 (m, 2 H, linker CH), 5.12 (br. m, 4 H, arms CH), 2.25–3.23 (br. m, 44 H, cyclen CH_2, arms CH_2CO and linker CH_2CO), 1.46 (br. m, 12 H, arms CH_3), 1.41 (br. m, 18 H, *t*Bu CH_3) ppm. ^{13}C NMR ($CDCl_3$, 125 MHz): δ = 170.6 and 170.5 (br., 6 C, arms and linker C=O), 156.3 (2 C, Boc C=O), 143.5 and 138.8 (br., 6 C, arms and linker $Ph_{(q)}$), 128.9, 128.5, 127.9, 126.8, 126.6 (30 C, arms and linker Ph), 80.1 (2 C, $Boc_{(q)}$), 60.3, 58.0, 57.2, 54.3, 53.2, 48.7 (br., 28 C, cyclen CH_2, arms CH_2, linker CH_2 and arms and linker CH), 28.8 (6 C, Boc CH_3), 22.3, 21.7 (4 C, amide arm CH_3) ppm. MS (ES^+) *m*/*z* 742.0 $[M + 2H]^{2+}$ 100%, 1481.8 $[M + H]^+$ 5%, 1503.8 $[M + Na]^+$ 3%. HRMS (ES^+) *m*/*z* found 1481.906 $[M + H]^+$ $C_{84}H_{117}O_{10}N_{14}$ requires 1481.907.

Ligand L^{2b}: A colourless solution of **2b** (0.038 g, 0.026 mmol) in DCM/TFA (2:1, 3 mL) was stirred for 12 h in a sealed flask. The resultant yellow tinged solution was dried under reduced pressure to yield the TFA salt as a glassy yellow solid, in quantitative yield. ^1H NMR (CD_3CN, 500 MHz): δ = 7.93 (d, *J* = 9.0 Hz, 1 H, linker amide NH), 7.86 (d, *J* = 9.0 Hz, 1 H, linker amide NH), 7.00–7.59 (m, 34 H, arm and linker Ar and arm NH), 5.32 (m, 2 H, linker CH), 5.08 (m, 1 H, amide arm CH), 4.90 (m, 1 H, amide arm CH), 4.77 (m, 1 H, amide arm CH), 4.66 (m, 1 H, amide arm CH), 2.45–3.62 (m, 44 H, cyclen CH_2, arm CH_2 and linker CH_2), 1.49, 1.44, 1.22 (m, 12 H, arm CH_3) ppm. ^{13}C NMR (CD_3CN, 125 MHz): δ = 171.2, 170.8 (4 C, arms C=O), 163.6, 163.5 (2 C, linker C=O), 159.7 (q, 4 C, TFA C=O), 144.8, 144.3 (4 C, arm $Ar_{(q)}$), 139.5, 139.2 (2 C, linker $Ar_{(q)}$), 129.8, 129.5, 129.4, 129.2, 129.1, 128.1, 128.0, 127.1 (30 C, arm and linker Ar), 116.4 (q, 4 C, TFA CF_3), 58.8 (2 C, linker CH), 47.0–56.6 (br. m, 22 C, cyclen CH_2, linker CH_2, arm CH), 44.0 (4 C, arm CH_2), 22.9, 22.6, 22.1, 22.0 (4 C, arm CH_3) ppm. MS (ES^+) *m*/*z* 641.6 $[M + 2H]^{2+}$ 100%. HRMS (ES^+) *m*/*z* found 641.4048 $[M + 2H]^{2+}$ $C_{74}H_{102}O_6N_{14}$ requires 641.4048.

$[Eu_2{\cdot}L^{2b}(H_2O)_4]Cl_6{\cdot}xH_2O$: Ligand L^{2b} as its TFA salt (0.019 g, 0.015 mmol, molar mass of ligand as its free base used) and $Eu(OTf)_3$ (0.053 g, 0.088 mmol) in dry MeCN (1.75 mL) were heated at reflux for 72 h under argon. The solution was cooled to room temperature and solvent removed under reduced pressure. The crude material was purified as described above to yield the desired product as a white solid (10 mg, 0.005 mmol, 33%). MS (ES^+; excess ammonium acetate) *m*/*z* 567.3 $[M + 2CH_3CO_2 – H]^{3+}$ 100%, 850.5 $[M + 2CH_3CO_2 – 2H]^{2+}$ 50%. HRMS (ES^+, + NH_4OAc) *m*/*z* found 849.3222 $[M + 2CH_3CO_2 – 2H]^{2+}$ $C_{78}H_{104}O_{10}N_{14}{}^{151}Eu_2$ requires 849.3223; HPLC: t_R = 8.8 min.

$[Tb_2{\cdot}L^{2b}(H_2O)_4]Cl_6{\cdot}xH_2O$: Ligand L^{2b} as its TFA salt (0.008 g, 0.006 mmol, molar mass of ligand its free base used) and $TbCl_3{\cdot}6H_2O$ (0.014 g, 0.037 mmol) in dry MeOH (1 mL) were heated to reflux for 48 h under argon. The solution was cooled to room temperature and solvent removed under reduced pressure. The complex was isolated as described above to yield a white powder (0.007 g, 0.0036 mmol, 60%). MS (ES^+ excess ammonium acetate) *m*/*z* 572.3 $[M + 2CH_3CO_2 – H]^{3+}$ 83%, 857.6 $[M + 2CH_3CO_2 – 2H]^{2+}$ 100%. HRMS (ES^+, + NH_4OAc) *m*/*z* found 857.3284 $[M + 2CH_3CO_2 – 2H]^{2+}$ $C_{78}H_{104}O_{10}N_{14}{}^{159}Tb_2$ requires 857.3278; HPLC: t_R = 8.9 min.

$[Yb_2{\cdot}L^{2b}(OAc)_2]OAc_4{\cdot}xH_2O$: Ligand L^{2b} as its TFA salt (0.063 g, 0.049 mmol, molar mass of ligand its free base used) and $Yb(OAc)_3{\cdot}4H_2O$ (0.123 g, 0.29 mmol) in $MeOH/H_2O$ (2 mL, 50:50) were heated to reflux for 48 h, under argon. The complex was isolated as described above to yield a white solid (0.065 g, 0.031 mmol, 64%); m.p. 196–197 °C (dec.). MS (ES^+, excess ammonium acetate) *m*/*z* 581.6 $[M + 2CH_3CO_2 – H]^{3+}$ 100%, 872.0 $[M + 2CH_3CO_2 – 2H]^{2+}$ 15%. HRMS (ES^+) *m*/*z* found 869.3392 $[M + 2CH_3CO_2 – 2H]^{2+}$ $C_{78}H_{104}O_{10}N_{14}Yb_2$ requires 869.3391; HPLC: t_R = 8.7 min.

Acknowledgments

We thank Engineering and Physical Sciences Research Council (EPSRC), the Royal Society of Chemistry (RSC), the ESF Cost Action 38 for support and Professor T. Gunnlaugsson for access to facilities (CS).

[1] J. Rudovsky, M. Botta, P. Hermann, A. Koridze, S. Aime, *Dalton Trans.* **2006**, 2323.
[2] D. H. Powell, O. M. Ni Dhubhghaill, D. Pubanz, L. Helm, Y. S. Lebedev, W. Schlaepfer, A. E. Merbach, *J. Am. Chem. Soc.* **1996**, *118*, 9333.
[3] T. Gunnlaugsson, A. J. Harte, J. P. Leonard, M. Nieuwenhuyzen, *Chem. Commun.* **2002**, 2134; A. J. Harte, P. Jensen,

S. E. Plush, P. E. Kruger, T. Gunnlaugsson, *Inorg. Chem.* **2006**, *45*, 9465.
[4] S. J. A. Pope, A. M. Kenwright, V. A. Boote, S. Faulkner, *Dalton Trans.* **2003**, 3780.
[5] K. Nwe, M. Andolina, J. R. Morrow, *J. Am. Chem. Soc.* **2008**, *130*, 14861.
[6] J. I. Bruce, R. S. Dickins, L. J. Govenlock, T. Gunnlaugsson, S. Lopinski, M. P. Lowe, D. Parker, R. D. Peacock, J. J. B. Perry, M. Botta, S. Aime, *J. Am. Chem. Soc.* **2000**, *122*, 9674.
[7] D. Parker, R. S. Dickins, H. Puschmann, C. Crossland, J. A. K. Howard, *Chem. Rev.* **2002**, *102*, 1977.
[8] P. Atkinson, B. S. Murray, D. Parker, *Org. Biomol. Chem.* **2006**, *4*, 3166.
[9] a) P. Atkinson, Y. Bretonnière, D. Parker, G. Muller, *Helv. Chim. Acta* **2005**, *88*, 391; b) P. Atkinson, Y. Bretonnière, D. Parker, *Chem. Commun.* **2004**, 438.
[10] R. S. Dickins, S. Aime, A. S. Batsanov, A. Beeby, M. Botta, J. I. Bruce, J. A. K. Howard, C. S. Love, D. Parker, R. D. Peacock, H. Puschmann, *J. Am. Chem. Soc.* **2002**, *124*, 12697.
[11] R. S. Dickins, A. S. Batsanov, J. A. K. Howard, D. Parker, H. Puschmann, S. Salamano, *Dalton Trans.* **2004**, 70.
[12] T. Anai, E. Nakata, Y. Koshi, A. Ojida, I. Hamachi, *J. Am. Chem. Soc.* **2007**, *129*, 6232.
[13] L.-O. Palsson, R. Pal, B. S. Murray, D. Parker, A. Beeby, *Dalton Trans.* **2007**, 5726.
[14] J. A. Mosely, B. S. Murray, D. Parker, *Eur. J. Mass Spectrom.* **2009**, *15*, 145.
[15] a) G. Muller, *Dalton Trans.* **2009**, 9692; b) J. I. Bruce, D. Parker, R. D. Peacock, S. Lopinski, *Chirality* **2002**, *14*, 562.
[16] A. Beeby, I. M. Clarkson, R. S. Dickins, S. Faulkner, D. Parker, L. Royle, A. S. de Sousa, J. A. G. Williams, M. Woods, *J. Chem. Soc. Perkin Trans. 2* **1999**, 493.
[17] M. Botta, S. Aime, A. Barge, G. Bobba, R. S. Dickins, D. Parker, E. Terreno, *Chem. Eur. J.* **2003**, *9*, 2102.
[18] D. Parker, *Chem. Soc. Rev.* **2004**, *33*, 156.
[19] R. S. Dickins, D. Parker, J. I. Bruce, D. J. Tozer, *Dalton Trans.* **2003**, 1264.
[20] H. Donato, R. B. Martin, *Biochemistry* **1974**, *13*, 4575; C. L. A. Wang, T. Tao, J. Gergely, *J. Biol. Chem.* **1982**, *257*, 8372.
[21] R. A. H. Binstead, B. Jung, A. D. Zuberbühler, *SPECFIT/32 Global Analysis System*, v.3.0, Spectrum Software Associates, Marlborough, MA, USA, 2000–**2005**.
[22] M. Maeder, A. D. Zuberbühler, *Anal. Chem.* **1990**, *62*, 2220.

Received: March 1, 2010
Published Online: May 6, 2010

